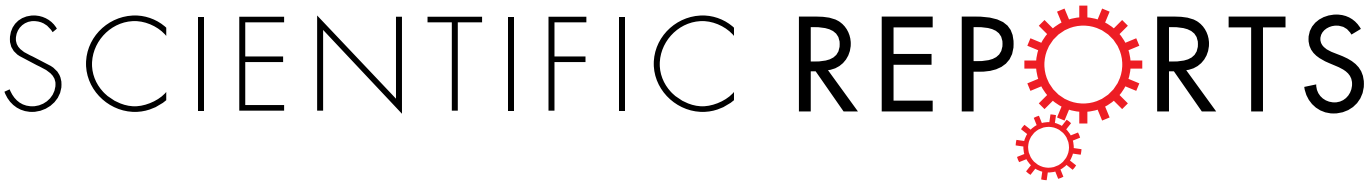

OPEN

Distributed atomic quantum information processing via optical fibers

Received: 25 January 2017
Accepted: 28 March 2017
Published online: 27 April 2017

Ming-Xing Luo[1,2], Hui-Ran Li[1] & Xiaojun Wang[3]

The qudit system may offer great flexibilities for quantum information processing. We investigate the possibility of realizing elementary quantum gates between two high-dimensional atoms in distant cavities coupled by an optical fiber. We show that highly reliable special swap gate is achievable by different detuning. The numerical simulation shows that the proposed elementary gate is robust against the atomic spontaneous decay, photon leakage of cavities and optical fibers by choosing the experimental parameters appropriately.

Non-classical electromagnetic fields have been described with the quantum mechanical for their special statistical properties, and experimentally realized with quantum optical experiments such as quadrature-squeezed and sub-Poissonian light fields[1–5]. These non-classical light fields may lead various interesting applications such as the enhanced measurement beyond the standard quantum limit set by vacuum fluctuations[4,6], or fundamental atomic processes through interaction with non-classical light[7–9].

A particularly interesting generation of non-classical light fields is related to cavity quantum electrodynamics, in which atoms interact strongly with a single quantized field mode of a cavity[10]. In both the microwave regimes[11–13] and optical regimes[8,14,15] the single atom cavity mode coupling strength may exceed spontaneous emission and cavity loss rates to produce observable effects of the coupled system. Rydberg atoms[16] and very high-Q superconducting cavities[17] are constructed in microwave experiments, where spontaneous emission and cavity damping are negligible on the time scale of the atom-field interaction. In optical regimes, the strong-coupling is reached via high-finesse cavities and very small cavity-mode volumes to avoid great spontaneous emission. The optical cavity is convenience because of direct transmission of light through the cavity mirrors, photon counting and homodyne detection[14,18,19].

The coherent evolution makes cavity quantum electrodynamics be favorable candidates for the realizations of photonic Fock states[20,21] and Schrödinger cat states[22,23]. Moreover, by using slowly decaying atomic levels (e.g., Rydberg atoms) or far-off-resonance atom-field interactions, atomic entanglements may be built[24–28]. The realizations of quantum gates between distant qubits in quantum optical settings have been recently investigated[27,28]. Such proposals are very promising and highly inventive. Serafini *et al.*[29] investigated the possibility of realizing effective quantum gates between two atoms in distant cavities coupled by an optical fiber. Zheng proposes an efficient scheme for quantum communication between two atoms trapped in distant cavities[30]. Moreover, flying single photons are also used for remote gates[31–35].

The purpose of this paper is to build the distributed quantum information processing using multilevel atoms. The qudit state (d-dimensional state) may offer greater flexibilities for storing quantum information, improving the channel capacity[36,37], reducing the implementation complexity of quantum gates[38–41], enhancing the information security[42–46] and exploring different quantum features[47–49]. There are various candidate systems for qudit states[50–53]. Unfortunately, few schemes have been proposed for implementing distributed quantum information processing based on qudit systems. Our scheme is based upon the adiabatic transformation of eigenstates of the atom-cavity system[54]. We firstly investigate the possibility of realizing deterministic gates between multi-level atoms in separate optical cavities, through a coherent resonant coupling mediated by an optical fiber. The only control required would be the synchronized switching on and off of the atom-field interactions in the distant cavities, which may be achievable through simple control pulses. Combined with single atomic transformations, the two-atom gate may be used to realize universal qudit quantum logic using recent circuit synthesis[55]. Finally,

[1]Information Security and National Computing Grid Laboratory, Southwest Jiaotong University, Chengdu, 610031, China. [2]Department of Physics, University of Michigan, Ann Arbor, MI, 48109, USA. [3]School of Electronic Engineering, Dublin City University, Dublin, 9, Ireland. Correspondence and requests for materials should be addressed to M.-X.L. (email: mxluo@home.swjtu.edu.cn) or H.-R.L. (email: hrlimm@163.com)

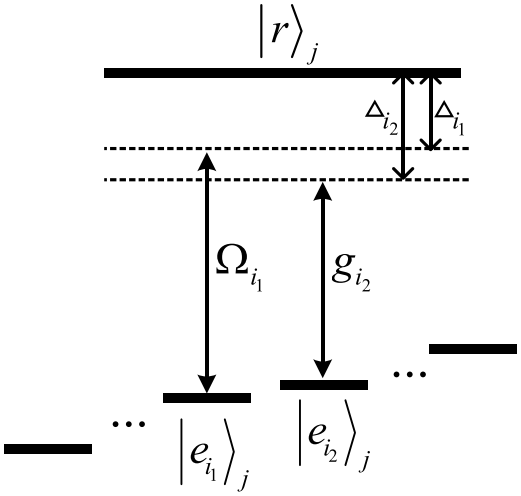

Figure 1. Involved atomic levels and transitions. The transition $|e_{i_1}\rangle_j \leftrightarrow |r\rangle$ of the j-th atom is coupled to the cavity mode with coupling constant g_j and detuning Δ_2. The transition $|e_{i_2}\rangle_j \leftrightarrow |r\rangle$ is driven by a classical field with Rabi frequency Ω_j and detuning Δ_1.

to show the possibility of these schemes, all the adiabatic conditions are considered. The numerical simulations show that our elementary gates are insensitive to the cavity decay, fiber loss, and atomic spontaneous emission. These gates can be constructed with high fidelity by choosing the parameters appropriately.

Result

Remote atomic model. The atomic level configuration is shown in Fig. 1. Each $d+1$-level atom has an excite state $|r\rangle$ and d ground states $|e_1\rangle$, …, $|e_d\rangle$. Two identical multi-level atoms are trapped in distant cavities connected by an optical fiber. The transition $|e_{i_2}\rangle \leftrightarrow |r\rangle$ of each atom is driven by a classical laser field with Rabi frequency Ω_{i_1}, while the transition $|e_{i_1}\rangle \leftrightarrow |r\rangle$ is driven by the cavity mode with coupling constant g_{i_2}. The mode number of the fiber is on the order of $l\overline{\nu}/2\pi c$, where l is the length of the fiber and $\overline{\nu}$ is the decay rate of the cavity field. When $l\overline{\nu}/2\pi c \leq 1$, there is only one fiber mode which essentially interacts with the cavity modes and the cavity-fiber coupling is described by the Hamiltonian as follows[29,30]

$$H_0 = \nu b(a_1^\dagger + a_2^\dagger) + H.c. \tag{1}$$

where b is the annihilation operator for the fiber mode, $a_j^\dagger$ is the creation operator for the j-th cavity mode, and ν is the cavity-fiber coupling strength.

Assume that the classical field and cavity mode are detuned from the respective transition by Δ_{i_1} and Δ_{i_2}. In the interaction picture, the Hamiltonian describes the following atom-field interaction

$$H_{int} = \sum_{j=1}^{2}\left(\Omega_{i_1} e^{i\Delta_{i_1}t}|r\rangle_{jj}\langle e_{i_1}| + g_{i_2} a_j e^{i\Delta_{i_2}t}|r\rangle_{jj}\langle e_{i_2}|\right) + H.c. \tag{2}$$

When $\Delta_{i_1}, \Delta_{i_2} \gg \Omega_{i_1}, g_{i_2}$, the excite state $|r\rangle$ can be adiabatically eliminated. It results in the following Hamiltonian

$$\begin{aligned} H_{int} &= -\sum_{j=1}^{2}\left(\eta_{i_1} e^{i\Delta_{i_1}t}|e_{i_1}\rangle_{jj}\langle e_{i_1}| + \zeta_{i_2} a_j^\dagger a_j |e_{i_2}\rangle_{jj}\langle e_{i_2}|\right) \\ &\quad + \lambda_{i_1 i_2}\left(a_j S_j^+ e^{i\delta_{i_1 i_2}t} + a^\dagger S_j^- e^{-i\delta_{i_1 i_2}t}\right) + H.c. \end{aligned} \tag{3}$$

where

$$\eta_{i_1} = \frac{\Omega_{i_1}^2}{\Delta_{i_1}},\ \zeta_{i_2} = \frac{g_{i_2}^2}{\Delta_{i_2}},\ \lambda_{i_1 i_2} = \frac{\Omega_{i_1} g_{i_2}}{2}\left(\frac{1}{\Delta_{i_1}} + \frac{1}{\Delta_{i_2}}\right) \tag{4}$$

with $\delta_{i_1 i_2} = \Delta_{i_2} - \Delta_{i_1}$, $S_j^+ = |e_{i_1}\rangle_{jj}\langle e_{i_2}|$ and $S_j^- = |e_{i_2}\rangle_{jj}\langle e_{i_1}|$. By introducing new Bosonic modes (see Method), the effective Hamiltonian is reduced to

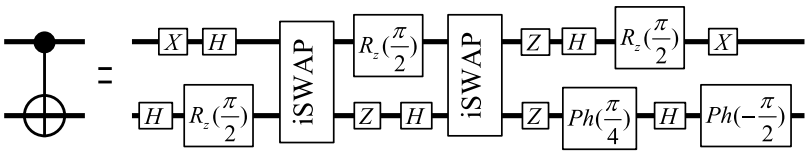

Figure 2. The circuit decomposition of the CNOT gate using the iSWAP gate and single qubit gates. H denotes the Hadamard gate. Z denotes the Pauli phase flip gate. $R_z(\theta)$ denotes the rotation along the z-axis on the Bloch sphere with the angle θ while $Ph(\theta)$ denotes the global phase gate with angle θ.

$$H_{eff} = \sum_{j=1}^{2} \mu_{i_1 i_2} |e_{i_1}\rangle_{jj} \langle e_{i_1}| - \chi_{i_1 i_2}(S_1^+ S_2^- + S_1^- S_2^+), \tag{5}$$

where

$$\mu_{i_1 i_2} = \frac{\lambda_{i_1 i_2}^2}{4}\left(\frac{2}{\delta_{i_1 i_2}} + \frac{2}{\delta_{i_1 i_2} - \sqrt{2}\nu} + \frac{2}{\delta_{i_1 i_2} + \sqrt{2}\nu}\right) + \zeta_{i_1}. \tag{6}$$

Distributed qudit computation. It is well-known that the qubit rotations and two-qubit CNOT gate are universal for synthesizing multi-qubit circuit. In this case, one only needs to construct CNOT gate using the system in Fig. 1. In fact, for two three-level atomic systems, each of them has two ground states $|e_1\rangle$, $|e_2\rangle$, and one excite state $|r\rangle$. Let atomic transition $|e_2\rangle \leftrightarrow |r\rangle$ be driven by a classical laser field with Rabi frequency Ω, while the transition $|e_1\rangle \leftrightarrow |r\rangle$ be driven by the cavity mode with coupling constant g. Assume that the classical field and the cavity mode are detuned from respective transition by Δ_1 and Δ_2. In the interaction picture, the Hamiltonian is simplified as

$$H_{eff} = -\mu \sum_{j=1}^{2} |e_1\rangle_{jj}\langle e_1| + \chi(S_2^+ S_3^- + S_2^- S_3^+) + H.c., \tag{7}$$

where $S_j^+ = |e_1\rangle_{jj}\langle e_2|$ and $S_j^- = |e_2\rangle_{jj}\langle e_1|$. After an evolving time t, it leads to a swapping gate

$$U_2(\mu, \chi) = \begin{pmatrix} e^{-i2\mu t} & 0 & 0 & 0 \\ 0 & e^{-i\mu t}\cos(\chi t) & ie^{-i\mu t}\sin(\chi t) & 0 \\ 0 & ie^{-i\mu t}\sin(\chi t) & e^{-i\mu t}\cos(\chi t) & 0 \\ 0 & 0 & 0 & 1 \end{pmatrix}. \tag{8}$$

Moreover, when $\mu t = (2k + 1)\pi$ and $\chi t = (2s + 1/2)\pi$ for some integers k and s, it reduces to the special SWAP gate

$$iSWAP = \begin{pmatrix} 1 & 0 & 0 & 0 \\ 0 & 0 & -i & 0 \\ 0 & -i & 0 & 0 \\ 0 & 0 & 0 & 1 \end{pmatrix}. \tag{9}$$

This gate may be used to generate CNOT gate, as shown in Fig. 2.

Qudit case. Now, we consider the qudit-based quantum computation. From previous result[55], the set of qudit gates $\{C_2[X_d], X_d\}$ is universal for synthesizing multi-qudit circuits. Here, X_d denotes the single qudit operation of $R_{ij}(\theta)$ or Z_d with the following forms

$$R_{ij}(\theta) = \begin{pmatrix} I_{i-1} & & & & \\ & \cos(\theta) & \cdots & \sin(\theta) & \\ & \vdots & \ddots & \vdots & \\ & -\sin(\theta) & \cdots & \cos(\theta) & \\ & & & & I_{d-j} \end{pmatrix},$$
$$Z_d(\theta) = \begin{pmatrix} e^{i\phi_1} & & & & \\ & e^{i\phi_2} & & & \\ & & \ddots & & \\ & & & e^{i\phi_{d-1}} & \\ & & & & e^{i\phi_d} \end{pmatrix}, \tag{10}$$

and $C_2[X_d]$ denotes the controlled qudit operation defined by

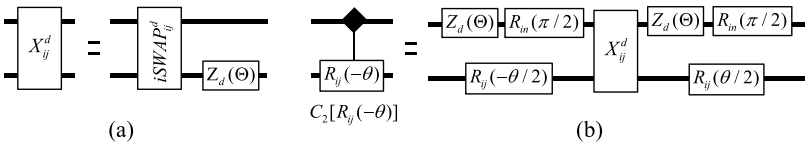

Figure 3. (**a**) The circuit decomposition of two-qudit gate X_{ij}^d defined in Eq. (15). (**b**) The circuit decomposition of two-qudit elementary gate $C_2[R_{ij}(\theta)]$. $R_{ij}^* = R_{ij}(\pi/2)Z_d(-\Theta)$, where $Z_d(-\Theta)$ is defined in Eq. (16) with $\Theta = (0_{d-1}, \pi)$.

$$C_2[X_d] = \begin{pmatrix} I_{d^2-d} & \\ & X_d \end{pmatrix}. \tag{11}$$

Since the qudit gate X_d may be realized assisted by the classical fields[54]. In the follow, our consideration is to realize $C_2[X_d]$ with the proposed atomic systems in Fig. 1. Firstly, we consider $C_2[R_{ij}]$ with two $d+1$-level atoms. Two cavity modes are coupled to the transition $|e_i\rangle \leftrightarrow |r\rangle$ of two atoms with the same detuning Δ_1. The transition $|e_j\rangle \leftrightarrow |r\rangle$ of two atoms is driven by classical fields with the same coupling coefficient Ω and detuning Δ_2. In this case, the effective Hamiltonian is simplified as

$$H_{eff} = -\mu(|e_i\rangle_{11}\langle e_i| + |e_i\rangle_{22}\langle e_i|) + \chi(S_2^+S_3^- + S_2^-S_3^+) + H.c., \tag{12}$$

where $S_k^+ = |e_j\rangle_{kk}\langle e_i|$ and $S_k^- = |e_i\rangle_{kk}\langle e_j|$. After a proper evolving time t ($\mu t = (2k+1)\pi$ and $\chi t = (2s + 1/2)\pi$ for some integers k and s), it leads to a special swapping gate as follows:

$$iSWAP_{ij}^d = -i|e_ie_j\rangle\langle e_je_i| - i|e_je_i\rangle\langle e_ie_j| + i.d.t., \tag{13}$$

where $i.d.t$ denotes the identity operation for all the other terms except to $|e_ie_j\rangle$ and $|e_je_i\rangle$ of two atoms. From the circuit in Fig. 3(a), it easily follows that

$$X_{ij}^d = (I_d \otimes Z_d(\Theta)) \times iSWAP_{ij}^d, \tag{14}$$

where X_{ij}^d is defined by

$$X_{ij}^d = |e_ie_i\rangle\langle e_ie_j| + |e_ie_j\rangle\langle e_ie_i| + i.d.t, \tag{15}$$

and $i.d.t$ denotes the identity operation for all the other terms except to $|e_ie_i\rangle$ and $|e_ie_j\rangle$ of two atoms, and $\Theta = (0_{i-1}, \pi/2, 0_{j-i-1}, \pi/2, 0_{d-j-1})$ with 0_k being a zero vector of k-dimension.

The two-qudit gate X_{ij}^d may be used to realize controlled qudit gate $C_2[X_d]$. From Fig. 3(b), note that

$$\begin{aligned} C_2[R_{ij}(-\theta)] = &\left(I_d \otimes R_{ij}\left(\frac{\theta}{2}\right)\right) \times \left(R_{in}\left(\frac{\pi}{2}\right)Z_d(\Theta) \otimes I_d\right) \times X_{ij}^d \\ &\times \left(R_{in}\left(\frac{\pi}{2}\right)Z_d(\Theta) \otimes I_d\right) \times \left(I_d \otimes R_{ij}\left(\frac{-\theta}{2}\right)\right), \end{aligned} \tag{16}$$

where $\Theta = (0_{d-1}, \pi)$. Now, for an elementary two-qudit gate $C_2[Z_d(\Theta)]$, from each $\Theta = (\theta_1, \theta_2, \ldots, \theta_d)$, $C_2[Z_d(\Theta)]$ may be decomposed into special two-qudit gates as follows

$$C_2[Z_d(\Theta)] = \prod_{(i,j)\in\mathcal{S}} C_2[Z_d(\Theta_{ij})], \tag{17}$$

where $\Theta_{ij} = (0_{i-1}, \theta_i, 0_{j-i-1}, \theta_j, 0_{d-j-1})$, and $\mathcal{S}$ denotes the integer-pair partition of the index set $\{1, 2, \ldots, d\}$. Now for simplicity, consider the subspace defined by $\{|e_ie_i\rangle, |e_ie_j\rangle, |e_je_i\rangle, |e_je_j\rangle\}$ while the other subspace is unchanged for the following evaluations. From the Hamiltonian H_{eff} in Eq. (12), after a proper evolution time t ($\chi t = 2k\pi$), it follows a two-qudit rotation

$$CZ_d(2\phi, \phi, \phi, 0) := e^{-i2\mu t}|e_ie_i\rangle\langle e_ie_i| + e^{-i\mu t}|e_ie_j\rangle\langle e_ie_j| + e^{-i\mu t}|e_je_i\rangle\langle e_je_i| + i.d.t. \tag{18}$$

with $\phi = -\mu t$. From Eqs (10) and (18), it follows that

$$\begin{aligned} CZ_d(2\phi,\ \phi,\ \pi,\ \phi) &:= \left(R_{jn}\left(\frac{\pi}{2}\right)\otimes I_d\right)\times CZ_d(2\phi,\ \phi,\ 0,\ \phi) \\ &\quad\times C_2\left[R_{ij}\left(-\frac{\pi}{2}\right)\right]\times\left(R_{jn}\left(\frac{\pi}{2}\right)\otimes I_d\right) \\ &= e^{-i2\mu t}|e_ie_i\rangle\langle e_ie_i| + e^{-i\mu t}\left|e_ie_j\right\rangle\left\langle e_ie_j\right| \\ &\quad -\left|e_je_i\right\rangle\left\langle e_je_i\right| + e^{-i\mu t}\left|e_je_j\right\rangle\left\langle e_je_j\right| + i.d.t. \end{aligned} \tag{19}$$

Similarly, one can get

$$\begin{aligned} CZ_d(\phi+\pi,\ 2\phi,\ \phi,\ 0) &:= \left(R_{in}\left(\frac{\pi}{2}\right)\otimes I_d\right)\times CZ_d(2\phi,\ \phi,\ \pi,\ \phi) \\ &\quad\times C_2\left[R_{ij}\left(-\frac{\pi}{2}\right)\right]\times\left(R_{in}\left(\frac{\pi}{2}\right)\otimes I_d\right) \\ &= e^{i(\pi-\mu t)}|e_ie_i\rangle\langle e_ie_i| + e^{-i2\mu t}\left|e_ie_j\right\rangle\left\langle e_ie_j\right| \\ &\quad + e^{-i\mu t}\left|e_je_i\right\rangle\left\langle e_je_i\right| + i.d.t. \end{aligned} \tag{20}$$

Two phase gates yield to

$$\begin{aligned} CZ_d(3\phi+\pi,\ 3\phi,\ \phi+\pi,\ \phi) &:= CZ_d(\phi+\pi,\ 2\phi,\ \phi,\ 0)\cdot CZ_d(2\phi,\ \phi,\ \pi,\ \phi) \\ &= e^{i(-3\mu t+\pi)}|e_ie_i\rangle\langle e_ie_i| + e^{-i3\mu t}\left|e_ie_j\right\rangle\left\langle e_ie_j\right| \\ &\quad + e^{i(\pi-\mu t)}\left|e_je_j\right\rangle\left\langle e_je_j\right| + e^{-i\mu t}\left|e_je_i\right\rangle\left\langle e_je_i\right| + i.d.t. \end{aligned} \tag{21}$$

From Eqs (10) and (21), it follows that

$$\begin{aligned} CZ_d(3\phi,\ 3\phi,\ \phi,\ \phi) &:= \left(R_{jn}\left(\frac{\pi}{2}\right)\otimes I_d\right)\times\left(R_{in}\left(\frac{\pi}{2}\right)\otimes I_d\right) \\ &\quad\times CZ_d(3\phi+\pi,\ 3\phi,\ \phi+\pi,\ \phi)\times C_2\left[R_{ij}\left(\frac{\pi}{2}\right)\right] \\ &\quad\times\left(R_{in}\left(\frac{\pi}{2}\right)\otimes I_d\right)\times C_2\left[R_{ij}\left(\frac{\pi}{2}\right)\right]\times\left(R_{in}\left(\frac{\pi}{2}\right)\otimes I_d\right) \\ &= e^{-i3\mu t}|e_ie_i\rangle\langle e_ie_i| + e^{-i3\mu t}\left|e_ie_j\right\rangle\left\langle e_ie_j\right| \\ &\quad + e^{-i\mu t)}\left|e_je_j\right\rangle\left\langle e_je_j\right| + e^{-i\mu t}\left|e_je_i\right\rangle\left\langle e_je_i\right| + i.d.t. \end{aligned} \tag{22}$$

From Eqs (10) and (22), it follows that

$$\begin{aligned} CZ_d(\phi,\ \phi,\ 3\phi,\ 3\phi) &:= \left(Z_d(\Theta)R_{ij}\left(\frac{\pi}{4}\right)R_{ij}\left(\frac{\pi}{4}\right)\otimes I_d\right) \\ &\quad\times CZ_d(3\phi,\ 3\phi,\ \phi,\ \phi)\times\left(Z_d(\Theta)R_{ij}\left(\frac{\pi}{4}\right)R_{ij}\left(\frac{\pi}{4}\right)\otimes I_d\right) \\ &= e^{-i\mu t}|e_ie_i\rangle\langle e_ie_i| + e^{-i\mu t}\left|e_ie_j\right\rangle\left\langle e_ie_j\right| \\ &\quad + e^{-i3\mu t)}\left|e_je_j\right\rangle\left\langle e_je_j\right| + e^{-i3\mu t}\left|e_je_i\right\rangle\left\langle e_je_i\right| + i.d.t. \end{aligned} \tag{23}$$

where $\Theta = (0_{j-1},\ \pi,\ 0_{d-j})$. From Eqs (27) and (28), we obtain

$$\begin{aligned} CZ_d(4\phi,\ 4\phi,\ 4\phi,\ 4\phi) &:= CZ_d(\phi,\ \phi,\ 3\phi,\ 3\phi)CZ_d(3\phi,\ 3\phi,\ \phi,\ \phi) \\ &= e^{-i4\mu t}|e_ie_i\rangle\langle e_ie_i| + e^{-i4\mu t}\left|e_ie_j\right\rangle\left\langle e_ie_j\right| \\ &\quad + e^{-i4\mu t)}\left|e_je_j\right\rangle\left\langle e_je_j\right| + e^{-i4\mu t}\left|e_je_i\right\rangle\left\langle e_je_i\right| + i.\ d.\ t., \end{aligned} \tag{24}$$

$$\begin{aligned} CZ_d(2\phi,\ 2\phi,\ -2\phi,\ -2\phi) &:= CZ_d(3\phi,\ 3\phi,\ \phi,\ \phi)CZ_d(-\phi,\ -\phi,\ -3\phi,\ -3\phi) \\ &= e^{-i2\mu t}|e_ie_i\rangle\langle e_ie_i| + e^{-i2\mu t}\left|e_ie_j\right\rangle\left\langle e_ie_j\right| \\ &\quad + e^{i2\mu t)}\left|e_je_j\right\rangle\left\langle e_je_j\right| + e^{i2\mu t}\left|e_je_i\right\rangle\left\langle e_je_i\right| + i.d.t., \end{aligned} \tag{25}$$

where $CZ_d(-\phi,\ -\phi,\ -3\phi,\ -3\phi)$ may be obtained by letting $-\phi = 2\pi - \phi = -\mu t$ for some t. Therefore, Eqs (23) and (25) lead to

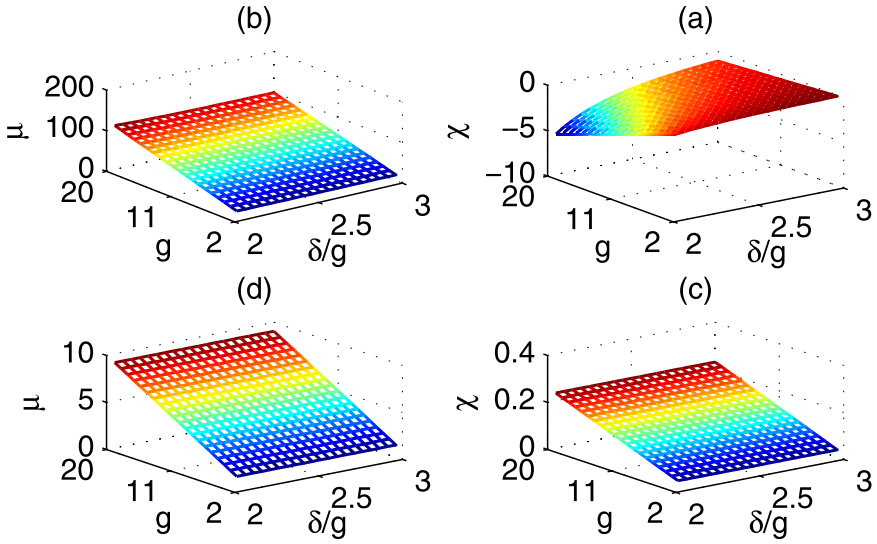

Figure 4. Two phase parameters μ and χ vias relative detuning δ/g and coupling strength g. (**a**) χ vias δ/g and g. (**b**) μ vias δ/g and g. Here, $\Delta_1 = 4g$, $\Delta_2 = 4g + \delta$, $\nu = g, \Omega = g$. $\mu > 0$ and $\chi < 0$ are useful for generating negative phases. (**c**) χ vias δ/g and g. (**d**) μ vias δ/g and g. Here, $\Delta_1 = 9g$, $\Delta_2 = 9g + \delta$, $\nu = 4g, \Omega = 3g$. Here, χ and μ are positive.

$$\begin{aligned} CZ_d(6\phi, 6\phi, 0, 0) &:= CZ_d(2\phi, 2\phi, -2\phi, -2\phi)CZ_d(4\phi, 4\phi, 4\phi, 4\phi) \\ &= e^{-i6\mu t}|e_i e_i\rangle\langle e_i e_i| + e^{-i6\mu t}|e_i e_j\rangle\langle e_i e_j| + i.d.t. \end{aligned} \tag{26}$$

Finally, the gate $C_2[Z_d(\Theta_{ij})]$ may be realized from the decomposition of $(R_{in}(\pi/2) \otimes I_d) \times CZ_{ij} \times (R_{in}(\pi/2) \otimes I_d)$ for different ϕ.

Effects of spontaneous decay and photon leakage. In this section, we study the influence of atomic spontaneous decay and photon leakage of the cavities and fibers. For convenience, we rewrite the interaction Hamiltonian under the dipole and rotating wave approximation. The master equation for the density matrices of the system is expressed as

$$\begin{aligned} \dot{\rho} &= -i[H, \rho] - \sum_j \Big\{ \frac{\kappa_{f_j}}{2}(b_j^\dagger b_j \rho - 2b_j \rho b_j^\dagger + \rho b_j^\dagger b_j) \\ &+ \frac{\kappa_{c_j}}{2}(a_j^\dagger a_j \rho - 2a_j \rho a_j^\dagger + \rho a_j^\dagger a_j) \\ &+ \sum_{i=1}^{d} \frac{\gamma_j^{ri}}{2}(\sigma_j^{rr}\rho - 2\sigma_j^{ir}\rho\sigma_j^{rx} + \rho\sigma_j^{rr}) \end{aligned} \tag{27}$$

where κ_{f_j} and κ_{c_j} denote the decay rates of the j-th cavity field and the j-th fiber mode, respectively, γ_j^{rx} denotes the spontaneous decay rate of the j-th atom from level $|r\rangle$ to $|e_i\rangle$, and $\sigma_k^{js} = |j\rangle_{kk}\langle s|(j, s = 1, \ldots, d)$ are the usual Pauli matrices. For the convenience, assume that $\kappa_{f_j} = \kappa_{c_s} = \kappa$ and $\gamma_j^{rx} = \gamma_a/d$ due to the equal probability transition of $|r\rangle \leftrightarrow |e_i\rangle$. In the follow, we will discuss the parameter conditions and experimental feasibility of the present scheme. With the choice of a scaling g, all the parameters can be reduced to the dimensionless units related to g.

To realize various rotations in Eqs (9) and (15), the rotation parameters χ and μ could achieve various values. In detail, consider the parameters of $\Delta_1 = 4g$, $\Delta_2 = 4g + \delta$, $\nu = g$ and $\Omega = 3g$. The rotation parameters χ and μ are shown in Fig. 4(a,b) respectively. It follows that μ may be changed largely while χ is negative. The ratio of μ and χ is changed from -110 to -20 in Fig. 5(a). Moreover, if another set of parameters $\Delta_1 = 9g$, $\Delta_2 = 9g + \delta$, $\nu = 4g$ and $\Omega = 3g$ are considered, the rotation parameters χ and μ are shown in Fig. 4(c,d) respectively. In this case, both of them are positive where their ratio is shown in Fig. 5(b).

For the first set of parameters shown in Fig. 4(a), all the adiabatic conditions $\nu_i \gg 0$ of $\nu_1 = \delta - \lambda$, $\nu_2 = |\delta - \sqrt{2}\nu| - \lambda/2$, $\nu_3 = \sqrt{2}\nu - \lambda/2$, and $\nu_4 = \sqrt{2}\nu - \eta/4$ are approximatively satisfied when g and δ/g are increased, as shown in Fig. 6(a–d). Here, $\nu_2 < 0$ should be avoided by choosing proper g and δ. If the second set of parameters shown in Fig. 4(c) are considered, the corresponding adiabatic conditions $\nu_i \gg 0$ of are greatly improved and shown in Fig. 6(f–h). Specially, in this case, all the $\nu_i > 0$ for all $g > 2$ and $\delta/g > 2$. It means that the adiabatic conditions may be satisfied under the weak coupling $g < 5$.

In order to complete the quantum applications, proper quantum gates should be realized using special phases $\phi = \mu t$ and $\psi = \chi t$ with proper evolution times. The phases ratio ϕ/ψ of all the gates including the iSWAP gate

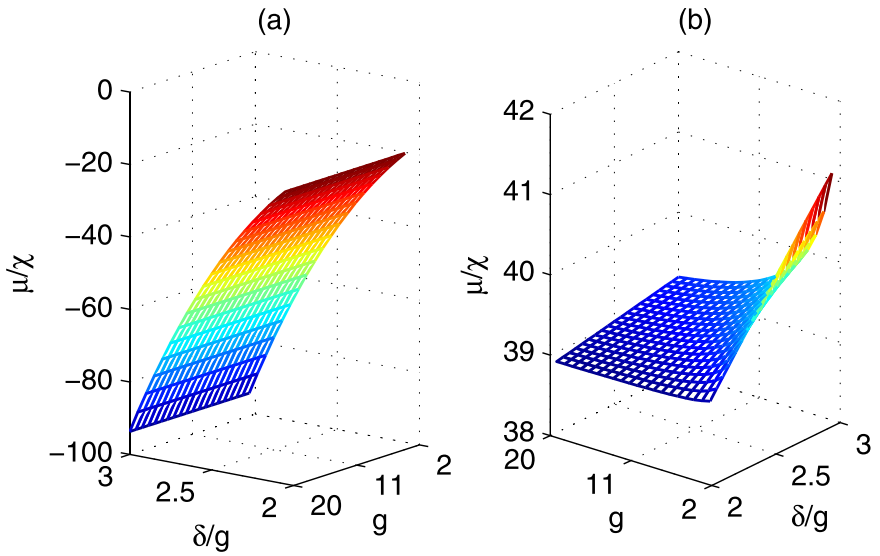

Figure 5. μ/χ vias δ/g and g. (**a**) $\Delta_1 = 4g$, $\Delta_2 = 4g + \delta$, $\nu = g$, $\Omega = g$; (**b**) $\Delta_1 = 9g$, $\Delta_2 = 9g + \delta$, $\nu = 4g$, $\Omega = 3g$.

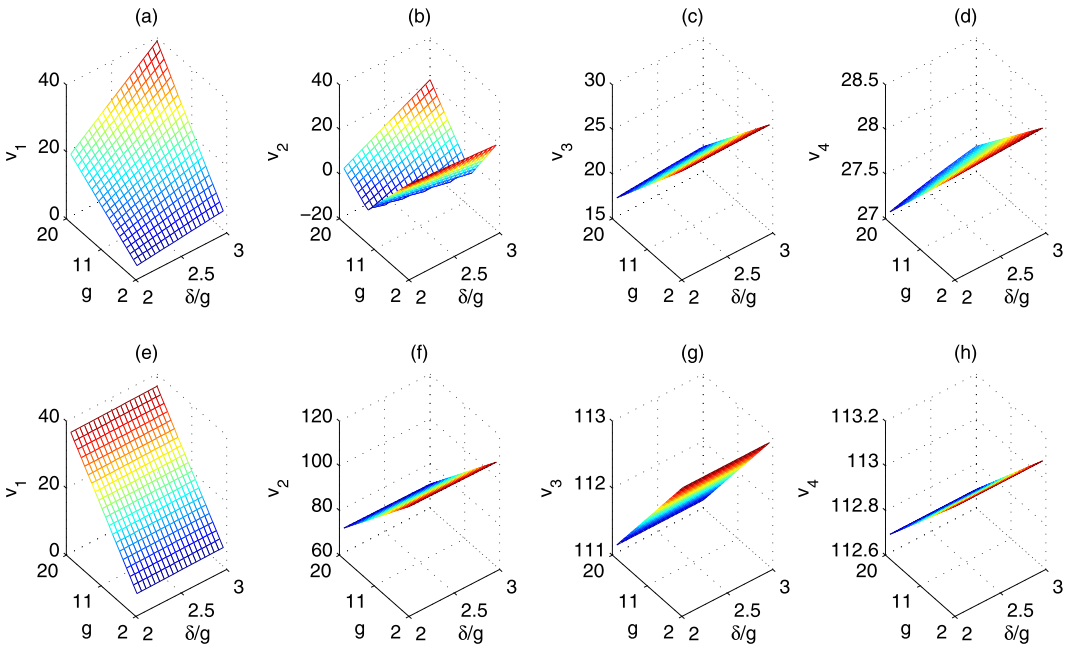

Figure 6. The adiabatic conditions vias δ/g and g. (**a**–**d**) Denote the first case in Fig. 4. (**e**–**h**) Denote the second case in Fig. 4. Here, $\nu_1 = \delta - \lambda$, $\nu_2 = |\delta - \sqrt{2}\nu| - \lambda/2$, $\nu_3 = \sqrt{2}\nu - \lambda/2$, and $\nu_4 = \sqrt{2}\nu - \eta/4$.

and inverse iSWAP gate are shown in Fig. 7(a,b). Combined with Fig. 5(a), these gates may be efficiently realized. Moreover, if another set of parameters $\Delta_1 = 9g$, $\Delta_2 = 9g + \delta$, $\nu = 4g$, and $\Omega = 3g$ are considered, the rotation parameters χ and μ are shown in Fig. 4(c,d) respectively. In this case, both of them are positive, and their ratio is shown in Fig. 5(b). The corresponding adiabatic conditions are improved and shown in Fig. 6(e,f). The phases ratio ϕ/ψ of different gates are shown in Fig. 7(c,d), which mean that the iSWAP gate and inverse iSWAP gate may be realized.

To consider atomic spontaneous emission and the decay of the Bosonic modes, let $\Gamma = \kappa = \gamma = 0.01g$, where Γ, κ, and γ are the decay rates for the atomic excited state, the cavity modes, and the fiber mode, respectively. The probability that the atoms undergo a transition to the excited state due to the off-resonant interaction with the classical fields is $P_1 = \Gamma/\Delta_1^2 < 0.01$ for both cases. Meanwhile, the probability that the three modes c_i are excited due to non-resonant coupling with the classical modes is

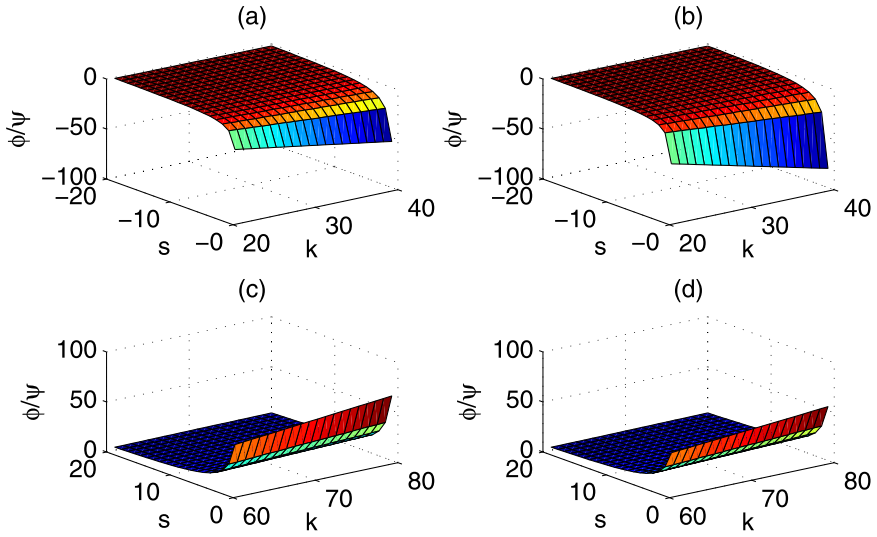

Figure 7. The phase ratio $\phi/\psi = (\mu t)/(\chi t)$ for the iSWAP gate and the inverse of iSWAP. (**a**,**b**) Denote the evolution times using the first set of parameters shown in Fig. 4(a). (**c**,**d**) Denote the evolution times using the second set of parameters shown in Fig. 4(c).

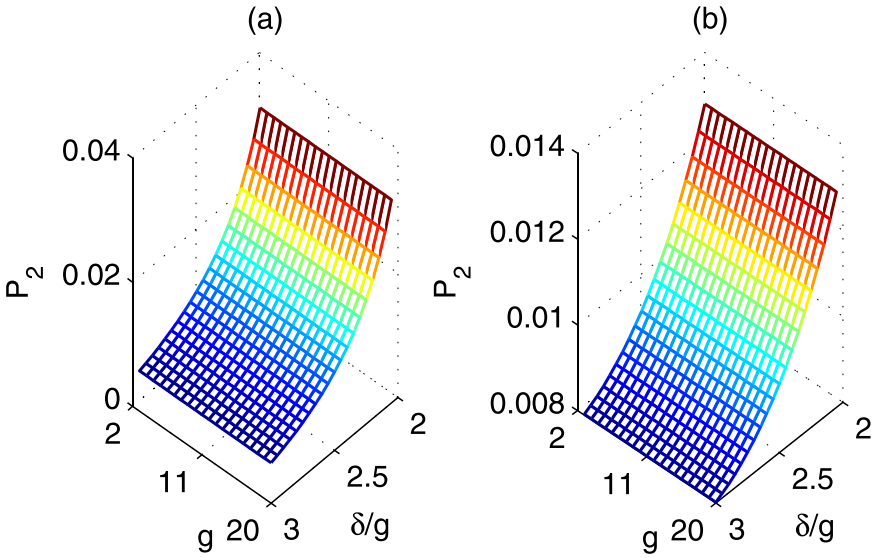

Figure 8. The probability P_2. (**a**) The first case; (**b**) The second case.

$$P_2 \approx \frac{\lambda^2}{4}\left[\frac{2}{\delta^2} + \frac{1}{(\delta - \sqrt{2}\nu)^2} + \frac{1}{(\delta + \sqrt{2}\nu)^2}\right]. \tag{28}$$

The P_2 is shown in Fig. 8 for two groups of parameters. The effective decoherence rates due to the atomic spontaneous emission and the decay of the Bosonic modes are $\Gamma' = P_1\Gamma < 10^{-4}g$ and $\kappa' = P_2\kappa < 0.35 \times 10^{-3}g$, respectively.

The fidelity of the iSWAP gate is defined by

$$F_{iSWAP} = \int Tr\left[\sqrt{\sqrt{\rho_o}\rho_i\sqrt{\rho_o}}\right] \tag{29}$$

over all possible states, where ρ_o denotes the real final density matrix while ρ_i denotes the ideal final density matrix. The fidelity of the iSWAP gate is shown in Fig. 9. For the small $g \approx 5.275$, the fidelity may be reached to 0.982 after the evolution time $t \approx 19.575$, see Fig. 9(a). For the large $g \approx 18.4$, the fidelity may be reached to 0.994 after the evolution time $t \approx 6.375$. The ideal iSWAP gate is achieved after eight Rabi-like oscillations, see Fig. 10. In the regime $\nu \gg g_i$ the fidelities of the gates have been consistently found to be essentially unaffected by fiber losses. In general, moreover, the direct effect of spontaneous emission proves to be more relevant than the indirect

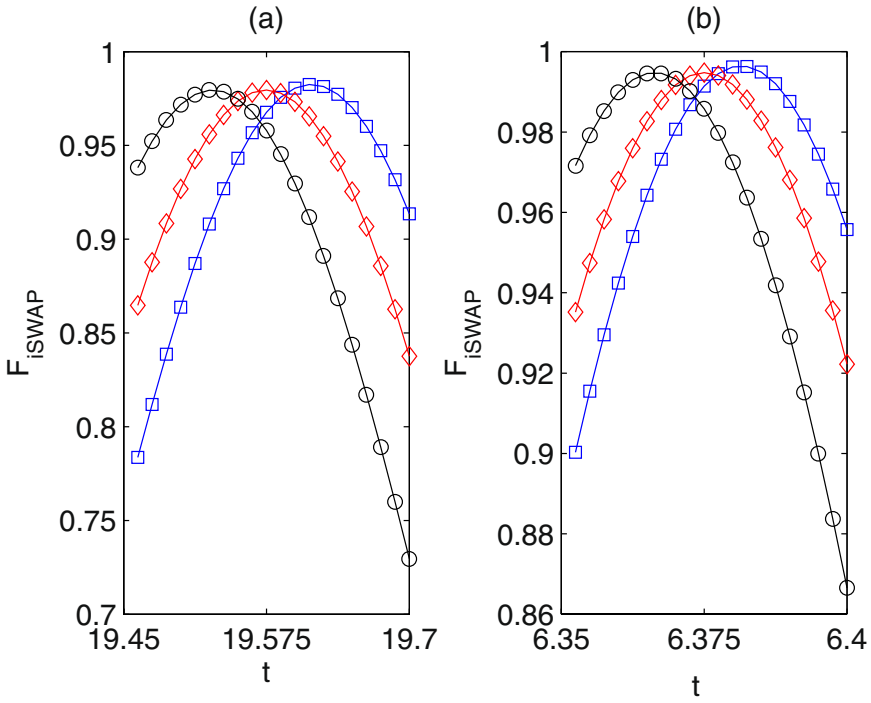

Figure 9. The average fidelity of the iSWAP gate vias g and evolution time. $\Delta_1 = 9g, \Delta_2 = 9g + \delta, \nu = 4g$, $\Omega = 2g$. (**a**) The diamonds refer to $g \approx 5.275$, the squares and the circle refer, respectively, to a variation of -0.025 and $+0.025$ of g. (**b**) The diamonds refer to $g \approx 18.4$, the squares and the circle refer, respectively, to a variation of -0.05 and $+0.05$ of g.

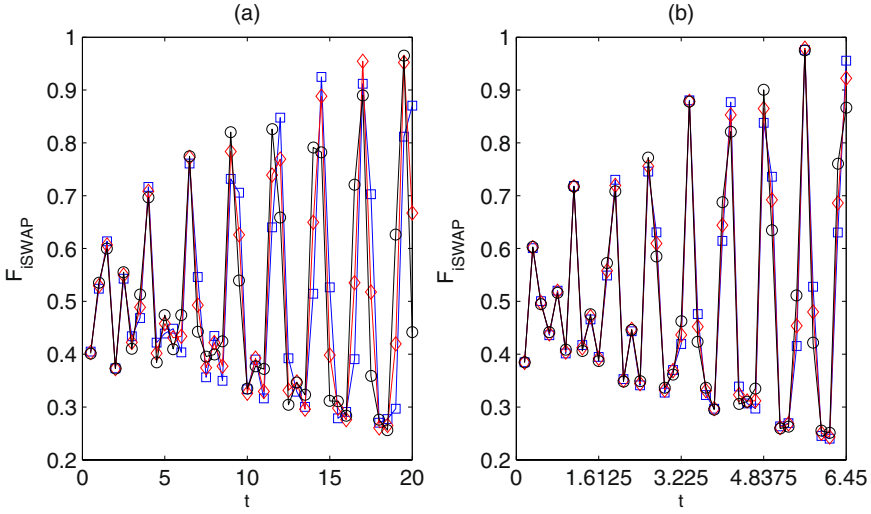

Figure 10. The fidelity of the iSWAP gate vias g and evolution time. $\Delta_1 = 9g, \Delta_2 = 9g + \delta, \nu = 4g, \Omega = 2g$. (**a**) The diamonds refer to $g \approx 5.275$, the squares and the circle refer, respectively, to a variation of -0.025 and $+0.025$ of g. (**b**) The diamonds refer to $g \approx 18.4$, the squares and the circle refer, respectively, to a variation of -0.05 and $+0.05$ of g.

effect of cavity losses. For the iSWAP gate with $\nu \approx 4g$ and $g \approx 5.275$, the maximum fidelity drops to $F \approx 0.958$ for $\kappa = \gamma = \beta = 0.002g$, see Fig. 11. If large coupling strength $g \approx 18.4$, the maximum fidelity drops to $F \approx 0.972$ for $\kappa = \gamma = \beta = 0.002g$. With lower decay rates $\approx 0.0002g$ the iSWAP gate is unaffected, while it may be spoiled if high rate $\approx 0.1g$ is considered. The spontaneous emission rates should be restricted for the fabrication of high-finesse optical cavities in experiment. Hyperfine ground levels of effective high level lambda systems could be candidates for such schemes. Take ^{87}Rb atoms as examples[56]. Three ground states may be defined by hyperfine atomic levels $|F = 1, m = -1\rangle, |F = 1, m = 0\rangle, |F = 1, m = 1\rangle$ of $5^2S_{1/2}$, while excited state may be

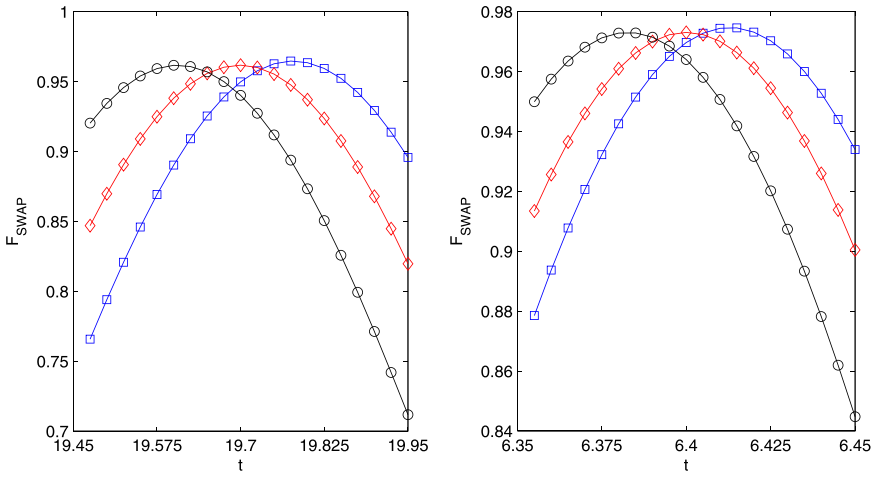

Figure 11. The fidelity of the iSWAP gate vias g and evolution time using master equation. $\Delta_1 = 9g$, $\Delta_2 = 9g + \delta$, $\nu = 4g$, $\kappa = \gamma = \beta = 0.002g$. $\Omega = 2g$. (**a**) The diamonds refer to $g \approx 5.275$, the squares and the circle refer, respectively, to a variation of -0.025 and $+0.025$ of g. (**b**) The diamonds refer to $g \approx 18.4$, the squares and the circle refer, respectively, to a variation of -0.05 and $+0.05$ of g.

defined by the hyperfine atomic level $|F = 1, m = 0\rangle$ of $5^2P_{1/2}$. Each atom can be made localized at a fixed position in each cavity with high Q for long time[56]. Recent experiment[57] has achieved the parameters $g/2\pi \approx 750$ MHz, $\kappa/2\pi \approx 2.62$ MHz, and $\gamma/2\pi \approx 3.5$ MHz in an ultrahigh-Q toroidal microresonators with the wavelength in the region 630~850 nm is predicatively achievable with the optical fiber decay rate 0.152 MHz[58]. By setting $\Omega_1 = \Omega_2 = 0.35g$, $\Delta_1 = 2.3g$, $\Delta_2 = 2.4g$, and $\nu = 0.8g$, we can obtain a iSWAP gate the fidelity about 9.21% with $\kappa \approx 0.0035g$ and $\gamma \approx 0.0046g$.

Conclusion

In conclusion, we have investigated the implementation of high-dimensional quantum computation for atoms trapped in distant cavities coupled by an optical fiber. The chosen ground states of each atom are coupled via the cavity mode and different classical fields in the Raman process. All the atoms do not undergo the real Raman transitions due to the large detuning while the atomic system is decoupled from the cavity modes and fiber modes. In the short fiber regime, reliable elementary gates could be reasonable even if imperfections (atomic spontaneous decay and photon leakage of the cavities and fibers) are considered. Let us also mention that, in the considered system, not only entangling and swap gates, but also perfect quantum state transfer is possible. Moreover, the proposed setup would also allow for entanglement preparation schemes between distributed atoms, and could useful in one-way quantum computation. These schemes would be useful for constructing large-scale and long-distance quantum computation or quantum communication networks.

Method

By introducing new Bosonic modes $c_1 = \frac{1}{\sqrt{2}}(a_1 - a_2)$, $c_2 = \frac{1}{2}(a_1 + a_2 + \sqrt{2}b)$ and $c_3 = \frac{1}{2}(a_1 + a_2 - \sqrt{2}b)$, the Hamiltonians H_0 may be rewritten as $H_0 = \frac{\nu}{\sqrt{2}}(c_2^\dagger c_2 - c_3^\dagger c_3)$. Take H_0 as the free Hamiltonian and perform the unitary transformation $U = e^{iH_0 t}$, it follows an efficient interaction Humiliation

$$
\begin{aligned}
H'_{int} \;=\; & \frac{\zeta_{i_2}}{4}(2c_1^\dagger c_1 + c_2^\dagger c_2)\sum_{j=1}^{2}\left|e_{i_2}\right\rangle_{jj}\left\langle e_{i_2}\right| - \sum_{j=1}^{2}\eta_{i_1}\left|e_{i_1}\right\rangle_{jj}\left\langle e_{i_1}\right| \\
& - \frac{1}{4}\Big\{2\lambda_{i_1 i_2}\Big[\sqrt{2}\,e^{i\delta_{i_1 i_2}t}c_1 + e^{i\left(\delta_{i_1 i_2}-\sqrt{2}\nu\right)t}c_2 + e^{i\left(\delta_{i_1 i_2}+\sqrt{2}\nu\right)t}c_3\Big]S_1^+ \\
& + 2\lambda_{i_1 i_2}\Big[\sqrt{2}\,e^{i\delta_{i_1 i_2}t}c_1 - e^{i\left(\delta_{i_1 i_2}-\sqrt{2}\nu\right)t}c_2 - e^{i\left(\delta_{i_1 i_2}+\sqrt{2}\nu\right)t}c_3\Big]S_2^+ \\
& + \zeta_{i_1 i_2}[\sqrt{2}\,e^{i\sqrt{2}\nu t}c_2^\dagger c_1 + e^{i\sqrt{2}\nu t}c_2^\dagger c_3 + \sqrt{2}\,e^{-i\sqrt{2}\nu t}c_3^\dagger c_1]\left|e_{i_2}\right\rangle_{11}\left\langle e_{i_2}\right| \\
& + \zeta_{i_1 i_2}[-\sqrt{2}\,e^{i\sqrt{2}\nu t}c_2^\dagger c_1 + e^{i\sqrt{2}\nu t}c_2^\dagger c_3 - \sqrt{2}\,e^{-i\sqrt{2}\nu t}c_3^\dagger c_1]\left|e_{i_2}\right\rangle_{22}\left\langle e_{i_2}\right|\Big\} + H.c.
\end{aligned}
\tag{30}
$$

The Hamiltonian describes multiple off-resonant Raman couplings for each atom induced by the classical field and the Bosonic modes c_1, c_2, c_3. If $\delta_{i_1 i_2} \gg \lambda_{i_1 i_2}$, $\left|\delta_{i_1 i_2} \pm \sqrt{2}\nu\right| \gg \lambda_{i_1 i_2}/2$ and $\sqrt{2}\nu \gg \lambda_{i_1 i_2}/2$, $\eta_{i_1}/4$, the Bosonic modes do not exchange quantum numbers with the atomic system. The off-resonant Raman coupling leads a Stark shift between the atoms.

Thus the effective Hamiltonian is defined by

$$
\begin{aligned}
H_{eff} &= \frac{\zeta_{i_2}}{4}(2c_1^{\dagger}c_1 + c_2^{\dagger}c_2)\sum_{j=1}^{2}\left|e_{i_2}\right\rangle_{jj}\left\langle e_{i_2}\right| - \sum_{j=1}^{2}\eta_{i_1}\left|e_{i_1}\right\rangle_{jj}\left\langle e_{i_1}\right| \\
&-\sum_{j=1}^{2}\frac{\lambda_{i_1i_2}^2}{4}\left\{\left[\frac{2}{\delta_{i_1i_2}}c_1c_1^{\dagger} + \frac{1}{\delta_{i_1i_2}-\sqrt{2}\nu}c_2c_2^{\dagger} + \frac{1}{\delta_{i_1i_2}+\sqrt{2}\nu}c_3c_3^{\dagger}\right]\left|e_{i_1}\right\rangle_{jj}\left\langle e_{i_1}\right|\right. \\
&+\left[\frac{2}{\delta_{i_1i_2}}c_1^{\dagger}c_1 - \frac{1}{\delta_{i_1i_2}-\sqrt{2}\nu}c_2^{\dagger}c_2 - \frac{1}{\delta_{i_1i_2}+\sqrt{2}\nu}c_3^{\dagger}c_3\right]\left|e_{i_2}\right\rangle_{jj}\left\langle e_{i_2}\right| \\
&+\frac{\zeta_{i_1i_2}^2}{32\sqrt{2}\mu}(c_2^{\dagger}c_2 - c_3^{\dagger}c_3)\left[\left(\left|e_{i_1}\right\rangle_{11}\left\langle e_{i_1}\right| + \left|e_{i_1}\right\rangle_{22}\left\langle e_{i_1}\right|\right)^2\right. \\
&\left.\left.+4\left(\left|e_{i_1}\right\rangle_{11}\left\langle e_{i_1}\right| - \left|e_{i_1}\right\rangle_{22}\left\langle e_{i_1}\right|\right)^2\right] - \chi_{i_1i_2}(S_1^{+}S_2^{-} + S_1^{-}S_2^{+})
\end{aligned}
\tag{31}
$$

where

$$
\chi_{i_1i_2} = \frac{\lambda_{i_1i_2}^2}{4}\left[\frac{2}{\delta_{i_1i_2}} - \frac{2}{\delta_{i_1i_2}-\sqrt{2}\nu} - \frac{2}{\delta_{i_1i_2}+\sqrt{2}\nu}\right] \tag{32}
$$

Since $2c_1^{\dagger}c_1, c_2^{\dagger}c_2, c_3^{\dagger}c_3$ commute with the Hamiltonian H_{eff}, the bosonic modes are unchanged if the vacuum states are applied.

References

1. Kimble, H. J. & Walls, D. F. Squeezed states of the electromagnetic field: Introduction to feature issue. *J. Opt. Soc. Am. B* **4**, 1449 (1987).
2. Kim, C. & Kumar, P. Quadrature-squeezed light detection using a self-generated matched local oscillator. *Phys. Rev. Lett.* **73**, 26–27 (1994).
3. Huck, A. *et al*. Demonstration of quadrature-squeezed surface plasmons in a gold waveguide. *Phys. Rev. Lett.* **102**, 246802 (2009).
4. Rempe, G., Schmidtkaler, F. & Walther, H. Observation of sub-Poissonian photon statistics in a micromaser. *Phys. Rev. Lett.* **64**, 2783–2786 (1990).
5. Mertz, J. *et al*. Observation of high-intensity sub-Poissonian light using an optical parametric oscillator. *Phys. Rev. Lett.* **64**, 2897–2900 (1990).
6. Bohnet, J. G. *et al*. Reduced spin measurement back-action for a phase sensitivity ten times beyond the standard quantum limit. *Nature Phot.* **8**, 731–736 (2014).
7. Rempe, G. *et al*. Optical bistability and photon statistics in cavity quantum electrodynamics. *Phys. Rev. Lett.* **67**, 1727 (1991).
8. Thompson, R. J., Rempe, G. & Kimble, H. J. Observation of normal-mode splitting for an atom in an optical cavity. *Phys. Rev. Lett.* **68**, 1132 (1992).
9. Boca, A. *et al*. Observation of the vacuum rabi spectrum for one trapped atom. *Phys. Rev. Lett.* **93**, 233603 (2004).
10. Wolf, E. (ed.) [Progress in Optics] [261–270] (North-Holland, Amsterdam, 1992).
11. Sandoghdar, V. V., Sukenik, C. I., Hinds, E. A. & Haroche, S. Direct measurement of the van der Waals interaction between an atom and its images in a micron-sized cavity. *Phys. Rev. Lett.* **68**, 3432–3435 (1992).
12. Bernardot, F. *et al*. Vacuum rabi splitting observed on a microscopic atomic sample in a microwave cavity. *Europhys. Lett.* **17**, 33–38 (2007).
13. Persson, E., Rotter, I., Stöckmann, H.-J. & Barth, M. Observation of resonance trapping in an open microwave cavity. *Phys. Rev. Lett.* **85**, 2478 (2000).
14. Birnbaum, K. M. *et al*. Photon blockade in an optical cavity with one trapped atom. *Nature* **436**, 87–90 (2005).
15. Colombe, Y. *et al*. Strong atom-field coupling for Bose-Einstein condensates in an optical cavity on a chip. *Nature* **450**, 272–276 (2007).
16. Saffman, M., Walker, T. G. & Mølmer, K. Quantum information with Rydberg atoms. *Rev. Mod. Phys.* **82**, 2313 (2010).
17. Hao, Y., Rouxinol, F. & LaHaye, M. D. Development of a broadband reflective T-filter for voltage biasing high-Q superconducting microwave cavities. *Appl. Phys. Lett.* **105**, 222603 (2014).
18. Wang, H., Goorskey, D. & Xiao, M. Controlling light by light with three-level atoms inside an optical cavity. *Optics Lett.* **27**, 1354–1356 (2002).
19. Wiseman, H. M. & Gj, M. Quantum theory of optical feedback via homodyne detection. *Phys. Rev. Lett.* **70**, 548–551 (1993).
20. Cirac, J. I., Blatt, R., Parkins, A. S. & Zoller, P. Preparation of Fock states by observation of quantum jumps in an ion trap. *Phys. Rev. Lett.* **70**, 762–765 (1993).
21. Hofheinz, M. *et al*. Generation of Fock states in a superconducting quantum circuit. *Nature* **454**, 310–314 (2008).
22. Monroe, C., Meekhof, D. M., King, B. E. & Wineland, D. J. A "Schrodinger cat" superposition state of an atom. *Science* **272**, 1131–1136 (1996).
23. Malbouisson, J. M. C. & Baseia, B. Higher-generation Schrödinger cat states in cavity QED. *J. Modern Optics* **46**, 2015–2041 (1999).
24. Duan, L. M. & Kimble, H. J. Efficient engineering of multiatom entanglement through single-photon detections. *Phys. Rev. Lett.* **90**, 253601 (2003).
25. Slodicka, L. *et al*. Atom-atom entanglement by single-photon detection. *Phys. Rev. Lett.* **110**, 083603 (2013).
26. Wang, D.-Y. *et al*. Scheme for generating the singlet state of three atoms trapped in distant cavities coupled by optical fibers. *Ann. Phys.* **360**, 228–236 (2015).
27. Jin, G. S., Li, S. S., Feng, S. L. & Zheng, H. Z. Generation of a supersinglet of three three-level atoms in cavity QED. *Phys. Rev. A* **71**, 034307 (2005).
28. Lin, G. W. *et al*. Generation of the singlet state for three atoms in cavity QED. *Phys. Rev. A* **76**, 014308 (2007).
29. Serafini, A., Mancini, S. & Bose, S. Distributed quantum computation via optical fibers. *Phys. Rev. Lett.* **96**, 010503 (2006).
30. Zheng, S. B. Quantum communication and entanglement between two distant atoms via vacuum fields. *Chin. Phys. B* **19**, 064204 (2010).
31. Huang, Y. F. *et al*. Experimental teleportation of a quantum controlled-NOT gate. *Phys. Rev. Lett.* **93**, 240501 (2004).
32. Huelga, S. F. *et al*. Remote implementation of quantum operations. *J. Opt. B Quantum Semiclass. Opt.* **7**, 1464–4266 (2005).

33. Wang, H. F., Zhu, A. D., Zhang, S. & Yeon, K. H. Optically controlled phase gate and teleportation of a controlled-not gate for spin qubits in a quantum-dot-microcavity coupled system. *Phys. Rev. A* **87**, 062337 (2013).
34. Luo, M. X., Li, H. R. & Wang, X. Teleportation of a controlled-NOT gate for photon and electron-spin qubits assisted by the nitrogen-vacancy center. *Quantum Inform. Comput.* **15**, 1397–1419 (2015).
35. Luo, M. X. & Wang, X. Universal remote quantum computation assisted by the cavity input-output process. *Proc. R. Soc. A* **471**, 20150274 (2015).
36. Fujiwara, M., Takeoka, M., Mizuno, J. & Sasaki, M. Exceeding the classical capacity limit in a quantum optical channel. *Phys. Rev. Lett.* **90**, 167906 (2003).
37. Schneeloch, J. *et al*. Violation of Continuous-Variable Einstein-Podolsky-Rosen Steering with Discrete Measurements. *Phys. Rev. Lett.* **108**, 959–960 (2012).
38. Ralph, T. C., Resch, K. & Gilchrist, A. Efficient Toffoli gates using qudits. *Phys. Rev. A* **75**, 022313 (2007).
39. Lanyon, B. P. *et al*. Manipulating biphotonic qutrits. *Phys. Rev. Lett.* **100**, 060504 (2008).
40. Lanyon, B. P. *et al*. Simplifying quantum logic using higher-dimensional Hilbert spaces. *Nature Phys.* **5**, 134–140 (2009).
41. Luo, M. X., Ma, S. Y., Chen, X. B. & Wang, X. Hybrid Toffoli gate on photons and quantum spins. *Sci. Rep.* **5**, 16716 (2015).
42. Nikolopoulos, G. M., Ranade, K. S. & Alber, G. Error tolerance of two-basis quantum-key-distribution protocols using qudits and two-way classical communication. *Phys. Rev. A* **73**, 032325 (2006).
43. Molina-Terriza, G. *et al*. Triggered qutrits for quantum communication protocols. *Phys. Rev. Lett.* **92**, 167903 (2004).
44. Bruß, D. & Macchiavello, C. Optimal eavesdropping in cryptography with three-dimensional quantum states. *Phys. Rev. Lett.* **88**, 127901 (2002).
45. Cerf, N. J., Bourennane, M., Karlsson, A. & Gisin, N. Security of quantum key distribution using *d*-level systems. *Phys. Rev. Lett.* **88**, 127902 (2002).
46. Walborn, S. P., Lemelle, D. S., Almeida, M. P. & Ribeiro, P. H. S. Quantum key distribution with higher-order alphabets using spatially encoded qudits. *Phys. Rev. Lett.* **96**, 090501 (2006).
47. Ivanov, P. A., Kyoseva, E. S. & Vitanov, N. V. Engineering of arbitrary $U(N)$ transformations by quantum Householder reflections. *Phys. Rev. A* **74**, 022323 (2006).
48. Vetesi, R., Pironio, S. & Brunner, N. Closing the detection loophole in Bell experiments using qudits. *Phys. Rev. Lett.* **104**, 060401 (2010).
49. Luo, M. X., Chen, X. B., Yang, Y. X. & Wang, X. Geometry of quantum computation with qudits. *Sci. Rep.* **4**, 4044 (2014).
50. O'ullivan-Hale, M. N., Khan, I. A., Boyd, R. W. & Howell, J. C. Pixel entanglement: experimental realization of optically entangled $d = 3$ and $d = 6$ qudits. *Phys. Rev. Lett.* **94**, 220501 (2005).
51. Moreva, E. V., Maslennikov, G. A., Straupe, S. S. & Kulik, S. P. Realization of four-level qudits using biphotons. *Phys. Rev. Lett.* **97**, 023602 (2006).
52. Fickler, R. *et al*. Quantum entanglement of high angular momenta. *Science* **338**, 640 (2012).
53. Fickler, R. *et al*. Interface between path and OAM entanglement for high-dimensional photonic quantum information. *Nature Commun.* **5**, 4502 (2014).
54. Parkins, A. S. *et al*. Quantum-state mapping between multilevel atoms and cavity light fields. *Phys. Rev. A* **51**, 1578–1591 (1995).
55. Luo, M. X. & Wang, X. Universal quantum computation with qudits. *Science China Phys., Mech. & Astr.* **57**, 1712–1717 (2014).
56. Mundt, A. B. *et al*. Coupling a single atomic quantum bit to a high finesse optical cavity. *Phys. Rev. Lett.* **89**, 103001 (2002).
57. Spillane, S. M. *et al*. Ultrahigh-Q toroidal microresonators for cavity quantum electrodynamics. *Phys. Rev. A* **71**, 013817 (2005).
58. Gordon, K. J., Fernandez, V., Townsend, P. D. & Buller, G. S. A short wavelength gigahertz clocked fiber-optic quantum key distribution system. *IEEE J. Quantum Electron.* **40**, 900 (2004).

Acknowledgements

We thank L. M. Duan and S. M. Tan. This work is supported by the National Natural Science Foundation of China (No. 61303039), Sichuan Youth Science and Technique Foundation (No. 2017JQ0048), Fundamental Research Funds for the Central Universities (No. 2682014CX095), Chuying Fellowship, CSC Scholarship, and EU ICT COST CryptoAction (No. IC1306).

Author Contributions

L.M.X. proposed the theoretical method. L.M.X. and L.H.R. wrote the main manuscript text. L.M.X. and W.X. reviewed the manuscript.

Additional Information

Competing Interests: The authors declare that they have no competing interests.

Publisher's note: Springer Nature remains neutral with regard to jurisdictional claims in published maps and institutional affiliations.